

Causal Policy Gradients

Thomas Spooner¹ Nelson Vadori¹ Sumitra Ganesh¹

Abstract

Policy gradient methods can solve complex tasks but often fail when the dimensionality of the action-space or objective multiplicity grow very large. This occurs, in part, because the variance on score-based gradient estimators scales quadratically with the number of targets. In this paper, we propose a causal baseline which exploits independence structure encoded in a novel action-target influence network. Causal policy gradients (CPGs), which follow, provide a common framework for analysing key state-of-the-art algorithms, are shown to generalise traditional policy gradients, and yield a principled way of incorporating prior knowledge of a problem domain’s generative processes. We provide an analysis of the proposed estimator and identify the conditions under which variance is guaranteed to improve. The algorithmic aspects of CPGs are also discussed, including optimal policy factorisations, their complexity, and the use of conditioning to efficiently scale to extremely large, concurrent tasks. The performance advantages for two variants of the algorithm are demonstrated on large-scale bandit and concurrent inventory management problems.

1. Introduction

Many sequential decision-making problems in the real-world have objectives that can be naturally decomposed into a set of conditionally independent targets. Control of water reservoirs, energy consumption optimisation, market making, cloud computing allocation, sewage flow systems, and robotics are but a few examples (Roijers et al., 2013). While many optimisation methods have been proposed (Mannor & Shimkin, 2004; Prashanth & Ghavamzadeh, 2016) — perhaps most prominently using Lagrangian scalarisation (Tessler et al., 2019) — multi-agent learning has emerged as a promising new paradigm for effective learn-

ing (Dusparic & Cahill, 2012).¹ In this class of algorithms, the multi-objective learning problem is cast into a centralised, co-operative stochastic game in which co-ordination is achieved through global coupling terms in each agent’s objective/reward function. For example, a grocer who must manage their stock could be decomposed into a collection of daemon agents that each manage a single type of produce, but are subject to global constraints on inventory. This approach has been shown to be very effective in a number of domains (Lee & Jangmin, 2002; Van Moffaert et al., 2014; Patel, 2018; Mannion et al., 2018; Wang et al., 2019), but presents both conceptual and technical issues.

The transformation of a multi-objective Markov decision process (MOMDP) (Roijers et al., 2013)² into a stochastic game is a non-trivial design challenge. In many cases there is no clear delineation between agents in the new system, nor an established way of performing the decomposition. What’s more, it’s unclear in many domains that a multi-agent perspective is appropriate, even as a technical trick. For example, the concurrent problems studied by Silver et al. (2013) exhibit great levels of homogeneity, lending themselves to the use of a shared policy which conditions on contextual information. The key challenge that we address in this paper is precisely how to scale these single-agent methods — specifically, policy gradients — in a *principled* way. As we shall see, this study reveals that existing methods in both single- and multi-agent multi-objective optimisation can be formulated as special cases of a wider family of algorithms we entitle *causal policy gradients*.

1.1. Contributions

1. We introduce *influence networks* as a framework for modelling causal relationships between actions and objectives in an MOMDP, and show how it can be combined with *policy factorisation* via graph partitioning.
2. We propose a *causal baseline* that exploits independence structures within a (factored) influence network, and show how this gives rise to a novel class of algorithms called *causal policy gradients*.

¹J.P. Morgan AI Research. Correspondence to: Thomas Spooner <thomas.spooner@jpmorgan.com>.

¹A related line of work has used multi-agent systems to learn a set of general value functions in tandem (Sutton et al., 2011).

²A similar construction by Altman (1999) instead considers explicit constraints. This is not the focus in this paper.

3. We show that CPGs *generalise traditional policy gradient estimators* and provide a common framework for analysing state-of-the-art algorithms in the literature including action-dependent baselines and counterfactual policy gradients.
4. *Minimum factorisation* is put forward as a principled way of applying CPGs, and is proven to always exist and be unique. We also discuss *conditioning vs. multiplicity* for task generalisation and reducing memory requirements in concurrent learning problems.
5. The final contribution is to illustrate the effectiveness of our approach over traditional estimators on two *high-dimensional benchmark domains*.

2. Background

A regular discrete-time Markov decision process (MDP) is a tuple $\mathcal{M} \doteq (\mathcal{S}, \mathcal{A}, \mathcal{R}, p, p_0)$, comprising: a *state space* \mathcal{S} , *action space* \mathcal{A} , and set of *rewards* $\mathcal{R} \subseteq \mathbb{R}$. The dynamics of the MDP are driven by an *initial state distribution* $s_0 \sim p_0(\cdot)$ and a stationary *transition kernel* with conditional probability density $(r_t, s_{t+1}) \sim p(\cdot, \cdot | s_t, \mathbf{a}_t)$ satisfying the Markov property, $p(r_t, s_{t+1} | h_t) = p(r_t, s_{t+1} | s_t, \mathbf{a}_t)$, for any history $h_t \doteq (s_0, \mathbf{a}_0, r_0, s_1, \dots, s_t, \mathbf{a}_t)$. Given an MDP, a (stochastic) policy, parameterised by $\theta \in \mathbb{R}^n$, is a mapping $\pi_\theta : \mathcal{S} \times \mathbb{R}^n \rightarrow \mathcal{P}(\mathcal{A})$ from states and weights to the set of probability measures on \mathcal{A} . The conditional probability density of an action \mathbf{a} is denoted by $\pi_\theta(\mathbf{a} | s) \doteq \mathbb{P}(\mathbf{a} \in d\mathbf{a} | s, \theta)$ and we assume throughout that π_θ is continuously differentiable with respect to θ . For a given policy, the *return* starting from time t is defined as the discounted sum of future rewards, $G_t \doteq \sum_{k=0}^T \gamma^k r_{t+k+1}$, where $\gamma \in [0, 1]$ is the discount rate and T is the terminal time (Sutton & Barto, 2018). *Value functions* express the expected value of returns generated from a given state or state-action pair under the MDP’s transition dynamics and policy π : $v_\pi(s) \doteq \mathbb{E}_\pi[G_t | s_t = s]$ and $q_\pi(s, \mathbf{a}) \doteq \mathbb{E}_\pi[G_t | s_t = s, \mathbf{a}_t = \mathbf{a}]$. The objective in *control* is to find a policy that maximises v_π for all states with non-zero measure under p_0 , denoted by the Lesbesgue integral

$$J(\theta) \doteq \mathbb{E}_{p_0}[v_{\pi_\theta}(s_0)] = \int_{\mathcal{S}} v_{\pi_\theta}(s_0) dp_0(s_0). \quad (1)$$

2.1. Policy Search

In this paper, we focus on policy gradient methods which optimise the parameters θ directly. This is achieved, in general, by performing gradient ascent on $J(\theta)$, for which Sutton et al. (2000) derived the differential form

$$\nabla_\theta J(\theta) = \mathbb{E}_{\pi_\theta, \rho_\pi} [(q_{\pi_\theta}(s, \mathbf{a}) - b(s)) \mathbf{z}], \quad (2)$$

where $\mathbf{z} \doteq \nabla_\theta \ln \pi_\theta(\mathbf{a} | s)$ is the policy’s score vector, $\rho_{\pi_\theta}(s) \doteq \int_{\mathcal{S}} \sum_{t=0}^{\infty} \gamma^t p(s_t = s | ds_0, \pi_\theta)$ denotes the (improper) discounted-ergodic occupancy measure, and $b(s)$

is a state-dependent baseline (or, control variate) (Peters & Schaal, 2006). Here, $p(s_t = s | s_0, \pi_\theta)$ is the probability of transitioning from $s_0 \rightarrow s$ in t steps under π_θ . Equation 2 is convenient for a number of reasons: 1. it is a score-based estimator (Mohamed et al., 2020); and 2. it falls under the class of stochastic approximation algorithms (Borkar, 2009). This is important as it means $q_\pi(s, \mathbf{a})$ may be replaced by *any* unbiased quantity, $\mathbb{E}_{\pi, \rho_\pi} [\psi(s, \mathbf{a})] \doteq q_\pi(s, \mathbf{a})$, while retaining convergence guarantees. It also implies that optimisation can be performed using stochastic gradient estimates, the standard variant of which is defined below.

Definition 2.1 (VPGs). The *vanilla policy gradient* estimator for target $\psi(s, \mathbf{a})$ and baseline $b(s)$ is denoted by

$$\mathbf{g}^V(s, \mathbf{a}) \doteq [\psi(s, \mathbf{a}) - b(s)] \mathbf{z} \quad (3)$$

where $\nabla_\theta J(\theta) = \mathbb{E}_{\pi_\theta, \rho_{\pi_\theta}} [\mathbf{g}^V(s, \mathbf{a})]$.

2.2. Factored (Action-Space) MDPs

In this paper, we consider the class of MDPs in which the action-space factors into a product, $\mathcal{A} \doteq \bigotimes_{i=1}^n \mathcal{A}_i = \mathcal{A}_1 \times \dots \times \mathcal{A}_n$, for some n . This is satisfied trivially when $n = 1$ and $\mathcal{A}_1 = \mathcal{A}$, but also holds in many common settings, such as $\mathcal{A} \doteq \mathbb{R}^n$, which factorises n times as $\bigotimes_{i=1}^n \mathbb{R}$. This is equivalent to requiring that actions, $\mathbf{a} \in \mathcal{A}$, are accessible in an elementwise fashion; without necessarily having \mathcal{A} be a vector space. For this purpose, we introduce the notion of partition maps which will be used throughout the paper.

Definition 2.2 (Partition Map). Define $\mathcal{X} \doteq \bigotimes_{i=1}^n \mathcal{X}_i$ and $J \subseteq [n]$, with $\mathcal{X}_J \doteq \bigotimes_{j \in J} \mathcal{X}_j$. Then, the partition map (PM) associated with (\mathcal{X}, J) , is given by the projection $\sigma : \mathcal{X} \rightarrow \mathcal{X}_J$, and its complement by $\bar{\sigma} : \mathcal{X} \rightarrow \mathcal{X}_{[n] \setminus J}$.

Partition maps are an extension of the canonical projections of the product topology, and are equivalent to the scope operator used by Tian et al. (2020). For example, if $(a_1, a_2, a_3) \doteq \mathbf{a} \in \mathcal{A} \doteq \mathbb{R}^3$ denotes a three-dimensional real action-space, then one possible PM is given by $\sigma(\mathbf{a}) = (a_1, a_3)$ with complement $\bar{\sigma}(\mathbf{a}) = (a_2)$. Note that there always exists of a unique inverse operation that recovers the original space; in this case, it would be expressed as $f((a_1, a_3), (a_2)) = (a_1, a_2, a_3)$.

3. Influence Networks

Consider an MOMDP with scalarised objective given by

$$J(\theta) \doteq \mathbb{E}_{p_0} \left[\psi(s, \mathbf{a}) \doteq \sum_{j=1}^m \lambda_j \psi_j(s, \sigma_j(\mathbf{a})) \right], \quad (4)$$

where $\lambda_j \in \mathbb{R}$ and each $\psi_j(s, \sigma_j(\mathbf{a}))$ denotes some target that depends on a single partition of the action components. Traditional MDPs can be seen as a special case in which

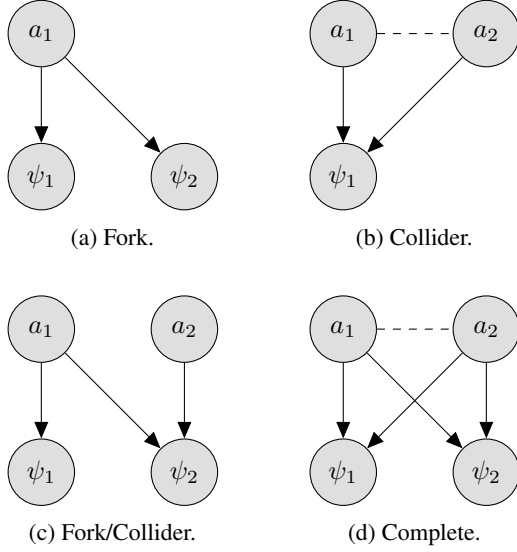


Figure 1. Influence network prototypes and action-target junction patterns (Pearl, 2009; Pearl & Mackenzie, 2018). Edges depict a dependence between factors $a_i \in \mathcal{A}$ and targets $\psi_j \in \Psi$, and the dashed lines a partition induced by the minimum factorisation.

$m = 1$, and $\psi = \psi_1 \doteq q_\pi(s, \mathbf{a})$. The vector $\psi(s, \mathbf{a})$ comprises the concatenation of all m targets and each partitioning is dictated by the *non-empty* maps $\sigma_j(\mathbf{a})$, the form of which is intrinsic to the MOMDP. For convenience, let us denote the collection of targets comprising $\psi(s, \mathbf{a})$ by

$$\Psi \doteq \{\psi_j : \psi(s, \mathbf{a}) = \langle \lambda, \psi(s, \mathbf{a}) \rangle\}. \quad (5)$$

Causal policy gradients are based on the observation that each factor of the action-space only *influences* a subset of the m targets. Take, for example, Figure 1c which depicts an instance of a (causal) influence network between a 2-dimensional action vector and a 2-dimensional target. The edges suggest that a_1 affects the value of both ψ_1 and ψ_2 , whereas a_2 only affects ψ_2 . This corresponds to an objective of the form $\lambda_1 \psi_1(s, a_1) + \lambda_2 \psi_2(s, \mathbf{a})$, where each goal’s domain derives from the edges of the graph. See below.

Definition 3.1 (Influence Network). A bipartite graph $\mathcal{G}(\mathcal{M}, \Psi) \doteq (I_{\mathcal{A}}, I_{\Psi}, E)$ is said to be the influence network of an MDP \mathcal{M} and target set Ψ if for $I_{\mathcal{A}} \doteq [|\mathcal{A}|]$ and $I_{\Psi} \doteq [|\Psi|]$, the presence of an edge, $e \in E$, between nodes $i \in I_{\mathcal{A}}$ and $j \in I_{\Psi}$ defines a causal relationship between the i^{th} factor of \mathcal{A} and the j^{th} target $\psi_j(s, \sigma_j(\mathbf{a}))$.

An influence network can be seen as a structural equation model (Pearl, 2009) in which each vertex in $I_{\mathcal{A}}$ has a single, unique parent which is exogenous and drives the randomness in action sampling, and each vertex in I_{Ψ} has parents only in the set $I_{\mathcal{A}}$ as defined by E . The structural equations along each edge $(i, j) \in E$ are given by the target functions themselves and the partition maps σ_j mirror the parents

of each node j . Some examples of influence networks are illustrated in Figure 1; see also the appendix. We now define the key concept of influence matrices.

Definition 3.2 (Influence Matrix). Let $K_{\mathcal{G}}$ denote the *bi-adjacency matrix* of an influence network \mathcal{G} , defined as the $|I_{\mathcal{A}}| \times |I_{\Psi}|$ boolean matrix with $K_{ij} = 1 \iff (i, j) \in E$ for $i \in I_{\mathcal{A}}$ and $j \in I_{\Psi}$.

Together, these definitions form a calculus for expressing the causal relationships between the factors of an action space and the targets of an objective of the form in Equation 4. We remark that, from an algorithmic perspective, we are free to choose between two representations: graph-based, or partition map-based. The duality between \mathcal{G} and K , and the set $\{\sigma_j : j \in I_{\Psi}\}$, is intrinsic to our choice of notation and serves as a useful correspondence during analysis.

3.1. Policy Factorisation

Influence networks contain all causal relationships between \mathcal{A} and Ψ , but policies are typically defined over groups of actions rather than the individual elements of \mathcal{A} . Consider, for example, a multi-asset trading problem in which an agent must quote buy and sell prices for each of n distinct assets (Guéant & Manziuk, 2019; Spooner & Savani, 2020). There is a natural partitioning between each pair of prices and the n sources of profit/loss, and one might therefore define the policy as a product of n bivariate Normal distributions as opposed to a full joint, or fully factored model. This choice over *policy factorisation* relates to the independence assumptions we make on the distribution π_{θ} for the sake of performance. Indeed, in the majority of the literature, policies are defined using an isotropic distribution (Wu et al., 2018) since there is no domain knowledge to motivate more complex covariance structure. We formalise this below.

Definition 3.3 (Policy Factorisation). A *policy factorisation*, $\Sigma \doteq \{\sigma_i^\pi : i \in |\Sigma|\}$, is a set of disjoint partition maps that form a complete partitioning over the action space.

The definition above provides a means of expressing *any* joint policy distribution over actions $\mathbf{a} \in \mathcal{A}$ in terms of PMs,

$$\pi_{\theta}(\mathbf{a} | s) \doteq \prod_{i=1}^n \pi_{i, \theta}(\sigma_i^\pi(\mathbf{a}) | s), \quad (6)$$

where each σ_i^π is an element of Σ . This corresponds to a transformation of the underlying influence network where the action vertices are grouped under the n policy factors and, for any $i, j \in [n]$, $i \neq j$, we have mutual independence: $\sigma_i^\pi(\mathbf{a}) \perp\!\!\!\perp \sigma_j^\pi(\mathbf{a})$. This is captured in the following concept.

Definition 3.4 (Factored Influence Network). For a given influence network \mathcal{G} and policy factorisation Σ , we define a *factored influence network*, \mathcal{G}_{Σ} , by replacing $I_{\mathcal{A}}$ with I_{Σ} , the set of partitioned vertices, and merge the corresponding

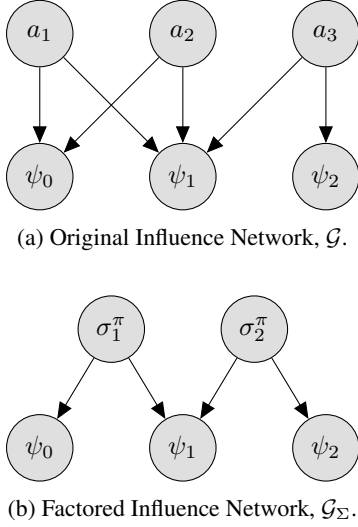


Figure 2. Influence network transformation under a Σ -factorisation with $\sigma_1^\pi(\mathbf{a}) \doteq (a_1, a_2)$ and $\sigma_2^\pi(\mathbf{a}) \doteq (a_3)$. Here, Σ corresponds to a minimum factorisation of the policy; i.e. $\Sigma = \Sigma^*$.

edges to give E_Σ . Similarly, denote by \mathbf{K}_Σ the influence matrix with respect to the Σ -factorisation.

Factored influence networks ascribe causal relationships between the policy factors in Equation 6 and the targets $\psi_j \in \Psi$. They play an important role in Section 4 and provide a refinement of Definition 3.1 which allows us to design more efficient algorithms. As an example, Figure 2 shows how one possible policy factorisation transforms an influence network \mathcal{G} into \mathcal{G}_Σ . Note that while the action nodes and edges have been partitioned into policy factors, the fundamental topology with respect to the attribution of influence remains unchanged.

4. Causal Policy Gradients

Causal policy gradients exploit factored influence networks by attributing each $\psi_j \in \Psi$ only to the policy factors that were probabilistically responsible for generating it; i.e. those with a connecting edge in the given \mathcal{G}_Σ . The intuition is that the extraneous targets in the objective do not contribute to learning, but do contribute towards variance. For example, it would be counter-intuitive to include ψ_2 of Figure 2b in the update for π_1 since it played no generative role. Naturally, by removing these terms from the gradient estimator, we can improve the signal to noise ratio and yield more stable algorithms. This idea can be formulated into a set of baselines which are defined and validated below.

Definition 4.1 (Causal Baselines). For a given \mathcal{G}_Σ , the *causal baselines* (CBs) are a family of $|\Sigma|$ control variates,

$$b_i^C(s, \bar{\sigma}_i^\pi(\mathbf{a})) \doteq [(1 - \mathbf{K}_\Sigma) \boldsymbol{\lambda} \circ \boldsymbol{\psi}(s, \mathbf{a})]_i, \quad (7)$$

where \circ denotes the Hadamard product.

Lemma 4.1. *Causal baselines are valid control variates.*

Proof. All proofs are provided in the appendix. ■

Causal baselines are related to the action-dependent baselines studied by Wu et al. (2018) and Tucker et al. (2018), as well as the methods employed by COMA (Foerster et al., 2018) and DRPGs (Castellini et al., 2020). Note, however, that CBs are distinct in two key ways: 1. they adhere to the structure of the influence network and account not only for policy factorisation, but also the target multiplicity of MOMDPs; and 2. unlike past work, the CBs were defined using an ansatz based on the structure implied by a given \mathcal{G}_Σ as opposed to explicitly deriving the $\arg \min$ of the variance; see Appendix D. This means that, unlike optimal baselines, CBs can be computed efficiently and thus yield practical algorithms. Indeed, this very fact is why the state-value function is used so ubiquitously in traditional actor-critic methods as a state-dependent control variate despite being sub-optimal. It follows that we can define an analogous family of methods for MOMDPs with negligible overhead.

Proposition 1 (CPGs). *Take a Σ -factored policy $\pi_\theta(\mathbf{a}|s)$ and $|\theta| \times |\Sigma|$ matrix of scores $\mathbf{S}(s, \mathbf{a})$. Then, for target vector $\boldsymbol{\psi}(s, \mathbf{a})$ and multipliers $\boldsymbol{\lambda}$, the CPG estimator*

$$\mathbf{g}^C(s, \mathbf{a}) \doteq \mathbf{S}(s, \mathbf{a}) \mathbf{K}_\Sigma \boldsymbol{\lambda} \circ \boldsymbol{\psi}(s, \mathbf{a}), \quad (8)$$

is unbiased; i.e. $\nabla_\theta J(\theta) = \mathbb{E}_{\pi_\theta, \rho_{\pi_\theta}} [\mathbf{g}^C(s, \mathbf{a})]$.

Proposition 1 above shows that the VPG estimator given in Definition 2.1 can be expressed in our causal calculus as $\mathbf{S} \mathbf{J} \boldsymbol{\lambda} \circ \boldsymbol{\psi}$, where \mathbf{J} is an all-ones matrix and, traditionally, $\boldsymbol{\psi} \doteq \mathbf{q}_\pi$; note that one can still include other baselines in Equation 8 such as v_π . In other words, Proposition 1 strictly generalises the policy gradient theorem (Sutton et al., 2000). We also see that both COMA (Foerster et al., 2018) and DRPGs (Castellini et al., 2020) are special cases in which the factorisation and target decomposition reflect the separation of agents with \mathbf{K}_Σ as a square, diagonal matrix.

4.1. Variance Analysis

The variance reducing effect of causal baselines comprises two terms: 1. a symmetric and strictly non-negative component which scales with the *second moments* of b_i^C ; and 2. an asymmetric term which scales with the *expected values* of b_i^C . This is shown in the following result.

Proposition 2 (Variance Decomposition). *Let \mathbf{g}_i denote a gradient estimate for the i^{th} factor of a Σ -factored policy π_θ (Equation 6). Then, $\Delta \mathbb{V}_i \doteq \mathbb{V}[\mathbf{g}_i^V] - \mathbb{V}[\mathbf{g}_i^C]$, satisfies*

$$\Delta \mathbb{V}_i = \alpha_i \mathbb{E}_{\bar{\sigma}_i^\pi(\mathbf{a})} [(b_i^C)^2] + 2\beta_i \mathbb{E}_{\bar{\sigma}_i^\pi(\mathbf{a})} [b_i^C], \quad (9)$$

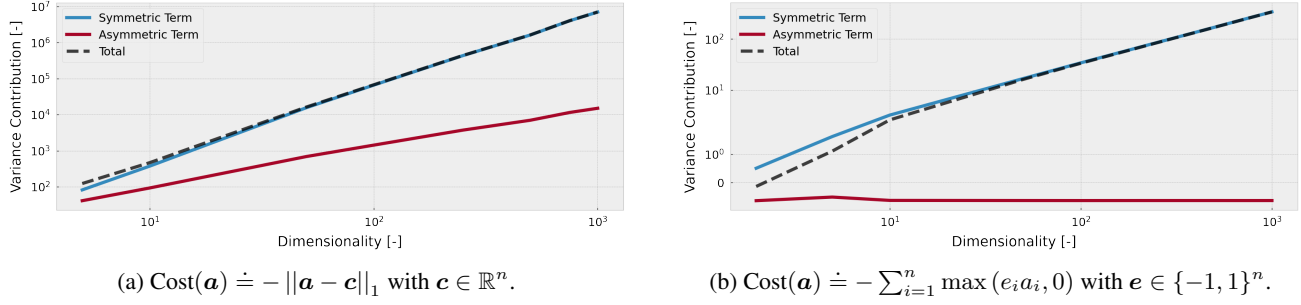


Figure 3. Variance decomposition on a symmetric log scale for two bandit problems as a function of action-space dimensionality. Each term was computed using Monte-Carlo estimation with 10^5 samples and taking the arithmetic mean across all policy factors.

where $\mathbf{z}_i \doteq \nabla_{\theta} \ln \pi_{i,\theta}(\mathbf{a} | s)$, $\alpha_i \doteq \mathbb{E}_{\sigma_i^{\pi}(\mathbf{a})}[\langle \mathbf{z}_i, \mathbf{z}_i \rangle] \geq 0$ and $\beta_i \doteq \mathbb{E}_{\sigma_i^{\pi}(\mathbf{a})}[\langle \mathbf{z}_i, \mathbf{z}_i \rangle (\psi + b_i^C)]$.

The first of these two terms acts as a “free lunch” by removing the targets that are not causally related to each factor. The asymmetric term, on the other hand, couples the adjusted target with the entries that were removed by the baseline. This suggests that asymmetry and covariance can have a regularising effect in VPGs that is not present in CPGs — a manifestation of the properties of control variates (Mohamed et al., 2020). Now, if we do not assume that the target functions are bounded, then the asymmetric term in Equation 9 can grow arbitrarily in either direction, but we typically require that rewards are restricted to some compact subset $\mathcal{R} \subset \mathbb{R}$ to avoid this. Below, we show that if a similar requirement holds for each target function — namely, that $\inf_{s, \mathbf{a}} \psi_j$ is well defined for each $\psi_j \in \Psi$ — then we can always construct a set of mappings that constrain (9) to be non-negative without biasing the gradient.

Corollary 4.1 (Non-Negative Variance Reduction). *Let $\psi(s, \mathbf{a})$ be of the form in Equation 4. If $\psi_j(s, \mathbf{a}) \geq \underline{\psi}_j$ for all $(s, \mathbf{a}) \in \mathcal{S} \times \mathcal{A}$ and $j \in [m]$, with $|\underline{\psi}_j| < \infty$, then there exists a linear translation, $\psi_i \rightarrow \psi_i - \sum_{j=1}^m \lambda_j \underline{\psi}_j$, which leaves the gradient unbiased but yields $\Delta \nabla_i \geq 0$.*

Interestingly, numerical experiments on a pair of continuum armed bandits suggest that this transformation is seldom necessary; see Figure 3. As the number of policy factors and targets grow, so too does the potential discrepancy in magnitude between the symmetric and asymmetric terms in Equation 9. The symmetric term starts to dominate even for small $|\Sigma|$. This is particularly prevalent when the influence matrix \mathbf{K}_{Σ} is very sparse and the baselines have wide coverage over Ψ . In other words, applying causal baselines when the influence network is very dense or even complete will not yield tangible benefits, but applying them to a problem with a rich causal structure will almost certainly yield a significant net reduction in variance.

5. CPG Algorithms

5.1. Minimum Factorisation

For many classes of fully-observable MDPs, any policy factorisation is theoretically viable: we can fully factor the policy such that each action dimension is independent of all others; or, at the other extreme, treat the policy as a full joint distribution over \mathbf{a} . This holds because, in many classes of (fully-observable) MDPs, there exists at least one deterministic optimal policy (Wiering & van Otterlo, 2012; Puterman, 2014). The covariance acts as a driver of exploration, and it’s initial value only affects the rate of convergence.³ As a result, most research uses an isotropic Gaussian with diagonal covariance to avoid the cost of matrix inversion. This poses an interesting question: is there an “optimal” policy factorisation, $\Sigma_{\mathcal{G}}^*$, associated with an influence network \mathcal{G} ? Below we offer a possible characterisation.

Definition 5.1 (Minimum Factorisation). A minimum factorisation (MF), $\Sigma_{\mathcal{G}}^*$, of an influence network, \mathcal{G} , is defined as a *minimum biclique vertex cover, disjoint amongst $I_{\mathcal{A}}$* .

It follows from Definition 5.1 that for any $\Sigma_{\mathcal{G}}^*$, each $\sigma_i \in \Sigma_{\mathcal{G}}^*$ is a biclique (i.e. complete bipartite subgraph) of the original influence network \mathcal{G} , and that the bipartite dimension is equal to the number of policy factors. For example, one can trivially verify that Figure 2b is an MF of the original graph; see also the reductions in Figure 1. From these properties we can even prove the following result:

Theorem 5.1. *The MF $\Sigma_{\mathcal{G}}^*$ always exists and is unique.*

We argue that minimum factorisation is highly intuitive and natural to the problem domains studied in this paper; see Section 6. It is also clear that a minimally factored policy will, generally, expose the minimum infimum bound on variance for a given influence network. This follows from the fact that an MF yields the greatest freedom to express covariance structure within each of the policy factors whilst

³We note that this is not true in general. In partially-observable MDPs and stochastic games, for example, the policy’s covariance structure impacts the set of possible solutions.

also maximising the symmetric term in Equation 9. In fact, when each action corresponds to a single unique target, the MF enjoys a linear lower bound on variance.

Complexity Computing a minimum vertex cover is an NP-complete problem in general (Karp, 1972), but the bipartite structure of influence networks and uniqueness property greatly reduces the complexity of identifying the MF. By König’s theorem, it can be related to a maximum matching problem for which there are efficient algorithms and is closely related to the constructions of Fleischer et al. (2009), suggesting that there exist simple, deterministic, polynomial-time algorithms for finding the MF.

5.2. Multiplicity vs. Conditioning

The policy factorisation defined in Equation 6 mirrors the independence relations of the influence network. The result is a *multiplicity* of statistically independent sub-policies which characterise the behaviour of the agent; or, indeed, multi-agent system. This formulation, however, can be inefficient in large and/or concurrent problems for two reasons: 1. each policy factor $\pi_{i,\theta}$ requires memory, which implies that $|\theta|$ grows (typically linearly) with $|\Sigma|$; and 2. the time-per-sample complexity of the full algorithm also requires $|\Sigma|$ iterations. We can alleviate this when dealing with intrinsically single-agent and (especially) concurrent problems (Silver et al., 2013) through conditioning, in which contextual features are fed as input to a single policy: that is, replace Equation 6 with *conditioned factors*,

$$\pi_{\theta}(\mathbf{a}|s) \doteq \prod_{i \in I_{\Sigma}} \pi_{\theta}(\sigma_i^{\pi}(\mathbf{a}) | s, c_i), \quad (10)$$

where c_i are contextual variables, and we require that the $|\text{Codomain}(\sigma_i^{\pi})|$ are equal for all $\sigma_i^{\pi} \in \Sigma$. This construction has the advantage of being able to generalise across tasks, requires only a single set of parameters, and exploits n -times as many gradient samples at each time step. This concept is equivalent to the parameter sharing of Foerster et al. (2016) and Gupta et al. (2017), and has been shown to be effective in many domains (Lan et al., 2019; Vadori et al., 2020).

6. Numerical Experiments

6.1. Search Bandit

Consider a continuum armed bandit with action space in \mathbb{R}^n and cost function: $\text{Cost}(\mathbf{a}) \doteq -\|\mathbf{a} - \mathbf{c}\|_1 - \lambda \zeta(\mathbf{a})$, where $\mathbf{c} \in \mathbb{R}^n$, $\lambda \geq 0$ and $\zeta : \mathcal{A} \rightarrow \mathbb{R}_+$ is a penalty function. This describes a search problem in which the agent must locate the centroid \mathbf{c} subject to an action-regularisation penalty. It abstracts away the prediction aspects of MDP settings, and allows us to focus only on scalability; note that this problem is closely related to the bandit studied by Wu et al. (2018) for the same purpose. In our experiments, the centroids were

initialised with a uniform distribution, $\mathbf{c} \sim \mathcal{U}(-5, 5)$ and were held fixed between episodes. The policy was defined as an isotropic Gaussian with fixed covariance, $\text{diag}(\mathbf{1})$, and initial location vector $\boldsymbol{\mu} \doteq \mathbf{0}$. The influence network was specified such that each policy factor, $\pi_{i,\theta}$ for $i \in [n]$, used a target $\psi_i(\mathbf{a}) \doteq -\Delta_i(a_i) - \lambda \zeta(a_i)$, with $\Delta_i(a) \doteq |a - c_i|$, amounting to a collection of n forks (Figure 1a). The parameter vector, $\boldsymbol{\mu}$, was updated at each time step, and the hyperparameters are provided in Appendix A.

Fully Decoupled We began by examining the case where $\lambda = 0$ and the co-ordinate axes were fully decoupled. For this, Figure 4 compares the performance of CPGs and VPGs in terms of the optimality gap after k iterations: $\mathbb{E}_{\pi^{(k)}}[\text{Cost}(\mathbf{a})] - \mathbb{E}_{\pi^*}[\text{Cost}(\mathbf{a})]$, where $\pi^{(k)}$ denotes the policy after k parameter updates, and $\pi^* \doteq \mathcal{N}(\mathbf{c}, \mathbf{1})$ is the optimal Gaussian policy with unit variance. We saw that CPGs facilitate much higher learning rates with a greatly decreased risk of divergence and optimisation errors. This was observed for action-spaces with dimensionality on the order $|\mathcal{A}| = 10^4$ which are completely intractable using traditional methods. To provide further intuition, we also analysed the number of time steps required by each method to reach a given optimality gap. We found that VPGs readily fail to reach a tolerance of 0.1 within the 5×10^5 iterations for learning rates greater than 0.5 and/or action spaces with more than 100 dimensions, and usually diverged entirely; see Figure 9 in the appendix. Conversely, CPGs demonstrated much better scalability, the only limit being that lower learning rates lead to inherently slower learning.

Penalty Coupling We then studied the impact of coupling terms in the cost function; i.e. $\lambda > 0$. For this, we considered a family of penalties taking the form of partially applied ℓ^2 norms: $\zeta_k(\mathbf{a}) \doteq \sqrt{\sum_{i=1}^k (a_i - c_i)^2}$, with $1 \leq k \leq n$. This set of functions allowed us to vary the penalty attribution across the n factors of \mathcal{A} . Figure 10 in the appendix, for example, demonstrates the performance advantage of CPGs for $k = n$ and $k = n/2$. In both cases, the improvement due to causal adjustment was found to be non-negative for every combination of learning rate and action space. This confirms that CPGs can indeed handle coupled targets and retains the variance reduction benefits that were explored in Section 4.1. As a more extreme example, we also considered the case where $k = n - 1$, in which all but the last action dimension were subject to a penalty. This is a particularly challenging setting for VPGs because the magnitude of the combined cost function is much greater than $\Delta_n(a_n)$, leading to an *aliasing* of the final component of the action vector in the gradient. The result, as exemplified in Figure 5, was that VPGs favoured reduction of overall error, and therefore exposed themselves to poor per-dimension performance; hence the increased noise in the a_n error process.

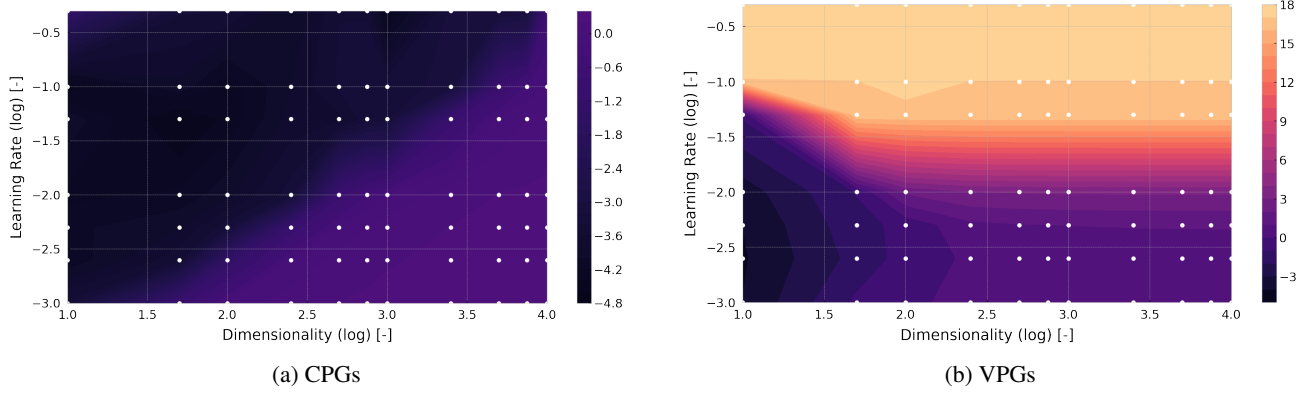


Figure 4. Mean optimality gap after 2×10^5 training iterations. The z -axis is given in a log scale and each point was computed from 16 random samples under the assumption of a Gamma distribution (optimality gap is lower bounded at zero).



Figure 5. Evolution of the squared error between a_n and c_n during learning for the search bandit with $k = n - 1$.

6.2. Apples and Oranges

The second domain is based on a real-world inventory management problem in which a merchant purchases goods from a set of wholesalers — say, apples and oranges — to sell at a marketplace. The vendor must learn two things: 1. to optimise their supply chain in line with current demand and the risk of spoilage (fruit is a perishable good); and 2. the optimal distribution of orders amongst the wholesalers who each offer a fixed (time-independent) price per item. The challenge for the agent is to ensure that it has sufficient inventory to meet demand whilst minimising waste. To model this, we assume that the demands for apples and oranges follow zero-inflated Poisson distributions with rates (ν_A, ν_O) and null probability κ ; i.e. the market only opens on days with good weather. Apples perish after 5 days, oranges after 4 days, and the agent sells them at market at fixed prices (u_A, u_O) . The action $\mathbf{a} \in \mathcal{A} \doteq [0, \bar{a}_A]^{|c_A|} \times [0, \bar{a}_O]^{|c_O|}$ corresponds to the agent’s order subject to caps on the quantities across the wholesalers, where the (strictly positive) costs per fruit are set at $\mathbf{c} \doteq (c_A, c_O)$, respectively. At each time step the demands are sampled and the quantities of sold fruit are removed from the agent’s inventories, $(\mathbf{H}_t^A, \mathbf{H}_t^O)$, going from freshest to oldest; note that $\mathcal{S} \doteq \mathbf{H}_t^A \times \mathbf{H}_t^O \in \mathbb{R}_+^9$, and $\mathbf{H}_0^A = \mathbf{H}_0^O \doteq \mathbf{0}$. The profit yield at each step is denoted by $Y_t \doteq Y_t^A + Y_t^O$ and we define the reward as $r_t \doteq Y_t - \langle \mathbf{c}, \mathbf{a}_t \rangle - \lambda P_{t+1}^2$. The latter term represents an

environmental penalty on wasted stock; i.e. $P_t \doteq P_t^A + P_t^O$ denotes the quantity of perished fruit between t and $t + 1$.

Learning Efficiency Our first experiment was designed to evaluate the benefits of CPGs and/or conditioned policies during learning. We considered three cases: 1. VPGs using a single isotropic Normal policy; 2. CPGs using separate isotropic Normal policies for apples and oranges, with rewards of $Y_t^A - \langle c_A, \mathbf{a}_t^A \rangle - \lambda P_t^2$ and $Y_t^O - \langle c_O, \mathbf{a}_t^O \rangle - \lambda P_t^2$, respectively; and 3. CPGs using the same split, but now using a pair of *conditioned* policies, one for each set of wholesalers (i.e. scalar output with one-hot encoding as context); see Appendix B. In all cases, we used the state-of-the-art combination of PPO (Schulman et al., 2017) and GAE (Schulman et al., 2015), with an *additional state-value baseline* and a 2-layer neural network for θ . The result, as illustrated in Figure 7, was that CPGs consistently outperformed VPGs. Interestingly, the conditioned policy, while more efficient in the early stages of learning, suffered from decreased asymptotic performance due to the additional complexity in the policy structure. This confirms that the “best” policy factorisation varies between problem domains.

Performance Comparison We then compared the performance of CPGs with VPGs (using non-conditional policies) for $\kappa \in [0.1, 0.2, 0.3]$ and $\lambda \in [0, 0.25, 0.5, 1]$. As shown in Figure 6, it was found that the solutions derived using a causal baseline yielded consistently higher total reward on average; e.g. for $\kappa = 0.1$ there was an increase of $\sim 10\%$, and for $\kappa = 0.2$ we saw an increase of $\sim 15\%$. The performance difference for $\kappa = 0.3$, however, was found to decay as λ increased. This aligns with the arguments presented in Section 4.1 — namely, that when coupling terms start to dominate, so the advantages of CPGs start to diminish. This indicates that for $(\kappa = 0.3, \lambda = 1)$, the optimal behaviour is mostly driven by λP_t^2 and scaling begins to have a significant effect. The particular choice of how to factorise an

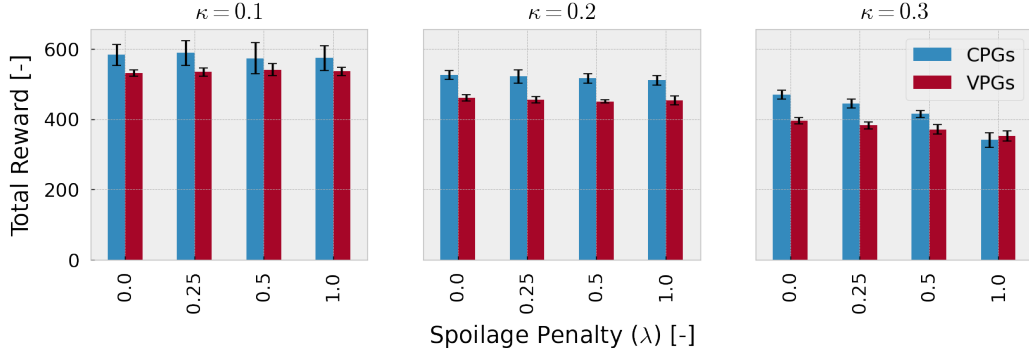


Figure 6. Average episodic reward for CPGs and VPGs in the apples and oranges environment as a function of κ and λ . Each point was computed using the mean over five randomised trials and the 95% confidence interval under a Normal assumption. All differences, excluding $(\kappa = 0.1, \lambda = 0.5)$ and $(\kappa = 0.3, \lambda = 1.0)$, are statistically significant to the 95% confidence level under a two-sample t-test.

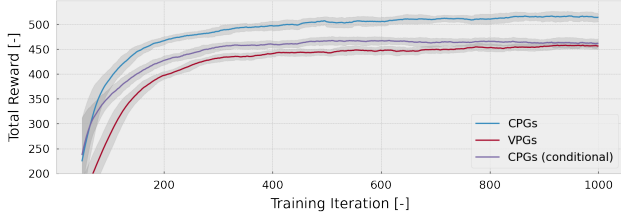


Figure 7. Rolling mean and standard deviation of episodic reward for the apples and oranges environment with $\kappa = 0.2$ and $\lambda = 0.5$.

influence network is evidently a key driver in performance.

7. Related Work

Variance reduction techniques in the context of policy gradient methods have been studied for some time. The seminal work of [Konda & Tsitsiklis \(2000\)](#), for example, was one of the earliest works that identified the use of a critic as beneficial for learning. Since then, baselines (or, control variates) have received much attention. In 2001, [Weaver & Tao](#) presented the first formal analysis of their properties, and later [Greensmith et al. \(2004\)](#) proved several key results around optimality. More recently, these techniques have been extended to include action-dependent baselines ([Thomas & Brunskill, 2017](#); [Liu et al., 2018](#); [Grathwohl et al., 2018](#); [Wu et al., 2018](#); [Foerster et al., 2018](#)). These, however, involve estimating gradient contributions which are often intractable. Various tricks have been proposed, and in some cases — e.g. with linear MDPs — there are analytical solutions, but there remains serious contention over the efficacy of *existing* approaches ([Tucker et al., 2018](#)). In a related but distinct strand of work, [Schulman et al. \(2015\)](#) also proposed generalised advantage estimation as a method for reducing variance in actor-critic methods with great success. Causal/graphical modelling has also seen past applications in RL ([Ghavamzadeh et al., 2015](#)). Perhaps most related is

the work of [Oliehoek et al. \(2008; 2012; 2019\)](#) who consider *influence*-based abstraction in multi-agent systems. There, local factorisation is used to exploit independence structures within a partially-observable stochastic game, leading to a characterisation of “local-form models”. Our proposed influence network is also related to, but distinct from, the action influence models introduced by [Madumal et al. \(2020\)](#) for explainability. There, the intention was to construct policies that can justify actions with respect to the observation space. Here, the intention was to exploit independence structure in MOMDPs for scalability and efficiency.

8. Conclusion

Causal policy gradients derive from the observation that many MOMDPs exhibit redundancy in their reward structure. Here, we have characterised this phenomenon using causal graphs, and demonstrated that conditional independence between factors of the action-space and the optimisation targets can be exploited in the form of a causal baseline. The resulting family of algorithms subsume many existing approaches in the literature. Our results in large-scale bandit and concurrent inventory management problems suggest that CPGs are highly suited to real-world problems, and may provide a way of scaling RL to domains that have hitherto remained intractable. What’s more, CPGs are compatible with other techniques that improve policy gradient performance. For example, they can be extended to use natural gradients by pre-multiplying [Equation 8](#) by the inverse Fisher information matrix ([Kakade, 2001](#)), and can even use additional baselines to reduce variance even further, as in [Section 6.2](#).

In future work we intend to address the following questions:

1. Can we infer/adapt the structure of influence networks?
2. Are there canonical structures within \mathcal{S} and \mathcal{K} ?
3. What are the deeper variance properties of CPGs?

Acknowledgements

The authors would like to acknowledge our colleagues Joshua Lockhart, Jason Long and Rui Silva for their input and suggestions at various key stages of the research.

This paper was prepared for informational purposes by the Artificial Intelligence Research group of JPMorgan Chase & Co and its affiliates (“J.P. Morgan”), and is not a product of the Research Department of J.P. Morgan. J.P. Morgan makes no representation and warranty whatsoever and disclaims all liability, for the completeness, accuracy or reliability of the information contained herein. This document is not intended as investment research or investment advice, or a recommendation, offer or solicitation for the purchase or sale of any security, financial instrument, financial product or service, or to be used in any way for evaluating the merits of participating in any transaction, and shall not constitute a solicitation under any jurisdiction or to any person, if such solicitation under such jurisdiction or to such person would be unlawful.

© 2021 JPMorgan Chase & Co. All rights reserved.

References

- Altman, E. *Constrained Markov Decision Processes*, volume 7. CRC Press, 1999.
- Borkar, V. S. *Stochastic Approximation: A Dynamical Systems Viewpoint*, volume 48. Springer, 2009.
- Castellini, J., Devlin, S., Oliehoek, F. A., and Savani, R. Difference Rewards Policy Gradients. *arXiv preprint arXiv:2012.11258*, 2020.
- Dusparic, I. and Cahill, V. Autonomic Multi-Policy Optimization in Pervasive Systems: Overview and evaluation. *TAAS*, 7(1):1–25, 2012.
- Fleischner, H., Mujuni, E., Paulusma, D., and Szeider, S. Covering Graphs with Few Complete Bipartite Subgraphs. *Theoretical Computer Science*, 410(21-23):2045–2053, 2009.
- Foerster, J., Farquhar, G., Afouras, T., Nardelli, N., and Whiteson, S. Counterfactual Multi-Agent Policy Gradients. In *Proc. of AAAI*, 2018.
- Foerster, J. N., Assael, Y. M., de Freitas, N., and Whiteson, S. Learning to Communicate with Deep Multi-Agent Reinforcement Learning. In *Proc. of NeurIPS*, pp. 2145–2153, 2016.
- Ghavamzadeh, M., Mannor, S., Pineau, J., and Tamar, A. Bayesian Reinforcement Learning: A Survey. *Foundations and Trends® in Machine Learning*, 8(5-6):359–483, 2015.
- Grathwohl, W., Choi, D., Wu, Y., Roeder, G., and Duvenaud, D. Backpropagation through the Void: Optimizing control variates for black-box gradient estimation. In *Proc. of ICLR*, 2018.
- Greensmith, E., Bartlett, P. L., and Baxter, J. Variance Reduction Techniques for Gradient Estimates in Reinforcement Learning. *JMLR*, 5:1471–1530, 2004.
- Guéant, O. and Manziuk, I. Deep Reinforcement Learning for Market Making in Corporate Bonds: Beating the Curse of Dimensionality. *Applied Mathematical Finance*, 26(5):387–452, 2019.
- Gupta, J. K., Egorov, M., and Kochenderfer, M. Cooperative Multi-Agent Control using Deep Reinforcement Learning. In *Proc. of AAMAS*, pp. 66–83, 2017.
- Kakade, S. M. A Natural Policy Gradient. *Proc. of NeurIPS*, 14:1531–1538, 2001.
- Karp, R. M. Reducibility Among Combinatorial Problems. In *Complexity of Computer Computations*, pp. 85–103. Springer, 1972.
- Konda, V. R. and Tsitsiklis, J. N. Actor-Critic Algorithms. In *Proc. of NeurIPS*, pp. 1008–1014, 2000.
- Lan, L., Li, Z., Guan, X., and Wang, P. Meta Reinforcement Learning with Task Embedding and Shared Policy. In *Proc. of IJCAI*, 2019.
- Lee, J. W. and Jangmin, O. A Multi-Agent Q-Learning Framework for Optimizing Stock Trading Systems. In *Proc. of DEXA*, pp. 153–162. Springer, 2002.
- Liu, H., Feng, Y., Mao, Y., Zhou, D., Peng, J., and Liu, Q. Action-Dependent Control Variates for Policy Optimization via Stein Identity. In *Proc. of ICLR*, 2018.
- Madumal, P., Miller, T., Sonenberg, L., and Vetere, F. Explainable Reinforcement Learning Through a Causal Lens. In *Proc. of AAAI*, volume 34, pp. 2493–2500, 2020.
- Mannion, P., Devlin, S., Duggan, J., and Howley, E. Reward shaping for knowledge-based multi-objective multi-agent reinforcement learning. *The Knowledge Engineering Review*, 33, 2018.
- Mannor, S. and Shimkin, N. A Geometric Approach to Multi-Criterion Reinforcement Learning. *JMLR*, 5:325–360, 2004.
- Mohamed, S., Rosca, M., Figurnov, M., and Mnih, A. Monte Carlo Gradient Estimation in Machine Learning. *JMLR*, 21(132):1–62, 2020.
- Oliehoek, F., Witwicki, S., and Kaelbling, L. Influence-Based Abstraction for Multiagent Systems. In *Proc. of AAAI*, volume 26, 2012.

- Oliehoek, F. A., Spaan, M. T., Vlassis, N., and Whiteson, S. Exploiting Locality of Interaction in Factored Dec-POMDPs. In *Proc. of AAMAS*, pp. 517–524, 2008.
- Oliehoek, F. A., Witwicki, S., and Kaelbling, L. P. A Sufficient Statistic for Influence in Structured Multiagent Environments. *arXiv preprint arXiv:1907.09278*, 2019.
- Patel, Y. Optimizing Market Making using Multi-Agent Reinforcement Learning. *arXiv preprint arXiv:1812.10252*, 2018.
- Pearl, J. *Causality*. Cambridge University Press, 2009.
- Pearl, J. and Mackenzie, D. *The Book of Why: The New Science of Cause and Effect*. Basic Books, 2018.
- Peters, J. and Schaal, S. Policy Gradient Methods for Robotics. In *Proc. of IEEE/RSJ*, pp. 2219–2225. IEEE, 2006.
- Prashanth, L. and Ghavamzadeh, M. Variance-Constrained Actor-Critic Algorithms for Discounted and Average Reward MDPs. *Machine Learning*, 105(3):367–417, 2016.
- Puterman, M. L. *[M]arkov Decision Processes: Discrete Stochastic Dynamic Programming*. John Wiley & Sons, 2014.
- Rojers, D. M., Vamplew, P., Whiteson, S., and Dazeley, R. A Survey of Multi-Objective Sequential Decision-Making. *JAIR*, 48:67–113, 2013.
- Schulman, J., Moritz, P., Levine, S., Jordan, M., and Abbeel, P. High-Dimensional Continuous Control using Generalized Advantage Estimation. *arXiv preprint arXiv:1506.02438*, 2015.
- Schulman, J., Wolski, F., Dhariwal, P., Radford, A., and Klimov, O. Proximal Policy Optimization Algorithms. *arXiv preprint arXiv:1707.06347*, 2017.
- Silver, D., Newnham, L., Barker, D., Weller, S., and McFall, J. Concurrent Reinforcement Learning from Customer Interactions. In *Proc. of ICML*, pp. 924–932, 2013.
- Spooner, T. and Savani, R. Robust Market Making via Adversarial Reinforcement Learning. In *Proc. of IJCAI*, pp. 4590–4596, 7 2020. Special Track on AI in FinTech.
- Sutton, R. S. and Barto, A. G. *Reinforcement Learning: An Introduction*. MIT Press, 2018.
- Sutton, R. S., McAllester, D. A., Singh, S. P., and Mansour, Y. Policy Gradient Methods for Reinforcement Learning with Function Approximation. In *Proc. NeurIPS*, pp. 1057–1063, 2000.
- Sutton, R. S., Modayil, J., Delp, M., Degris, T., Pilarski, P. M., White, A., and Precup, D. Horde: A Scalable Real-Time Architecture for Learning Knowledge from Unsupervised Sensorimotor Interaction. In *Proc. of AAMAS*, volume 2, pp. 761–768, 2011.
- Tessler, C., Mankowitz, D. J., and Mannor, S. Reward Constrained Policy Optimization. In *Proc. of ICLR*, 2019.
- Thomas, P. S. and Brunskill, E. Policy Gradient Methods for Reinforcement Learning with Function Approximation and Action-Dependent Baselines. *arXiv preprint arXiv:1706.06643*, 2017.
- Tian, Y., Qian, J., and Sra, S. Towards Minimax Optimal Reinforcement Learning in Factored Markov Decision Processes. *Proc. of NeurIPS*, 33, 2020.
- Tucker, G., Bhupatiraju, S., Gu, S., Turner, R., Ghahramani, Z., and Levine, S. The Mirage of Action-Dependent Baselines in Reinforcement Learning. In *Proc. of ICML*, volume 80, pp. 5015–5024, 10–15 Jul 2018.
- Vadori, N., Ganesh, S., Reddy, P., and Veloso, M. Calibration of Shared Equilibria in General Sum Partially Observable Markov Games. *Proc. of NeurIPS*, 33, 2020.
- Van Moffaert, K., Brys, T., Chandra, A., Esterle, L., Lewis, P. R., and Nowé, A. A Novel Adaptive Weight Selection Algorithm for Multi-Objective Multi-Agent Reinforcement Learning. In *Proc. of IJCNN*, pp. 2306–2314. IEEE, 2014.
- Wang, Y., Liu, H., Zheng, W., Xia, Y., Li, Y., Chen, P., Guo, K., and Xie, H. Multi-Objective Workflow Scheduling with Deep-Q-Network-Based Multi-Agent Reinforcement Learning. *Access*, 7:39974–39982, 2019.
- Weaver, L. and Tao, N. The Optimal Reward Baseline for Gradient-Based Reinforcement Learning. In *Proc. of UAI*, pp. 538–545, 2001.
- Wiering, M. and van Otterlo, M. *Reinforcement Learning: State-of-the-Art*, volume 12. Springer Science & Business Media, 2012.
- Wu, C., Rajeswaran, A., Duan, Y., Kumar, V., Bayen, A. M., Kakade, S., Mordatch, I., and Abbeel, P. Variance Reduction for Policy Gradient with Action-Dependent Factorized Baselines. In *Proc. of ICLR*, 2018.

A. Search Bandit

The search bandit is an interesting problem environment because, in many ways, it can emulate the learning process in arbitrary MDPs. This follows because, without loss of generality, we can always transform an MDP into a (possibly infinite) set of continuum multi-armed bandits, one occupying every unique state $s \in \mathcal{S}$. The question is how to define the cost function in order to achieve some form of equivalence. For example, if we consider deterministic policies, then we can clearly define the cost to be $\text{Cost}(\mathbf{a}) \doteq \|\mathbf{a} - \pi^*(s)\|_p$, for $p \geq 1$, and have the same solution set as given under the Bellman optimality. This is a powerful observation because it implies that the performance observed in the search bandit is likely to bound, in some form, the performance in the full MDP. This means that the results presented in [Section 6.1](#) provide strong evidence that CPGs will outperform VPGs for arbitrarily challenging MDPs.

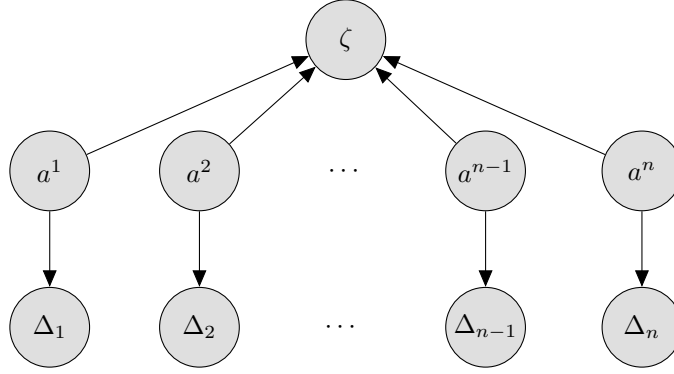


Figure 8. Influence network of the search bandit problem with optional coupling term.

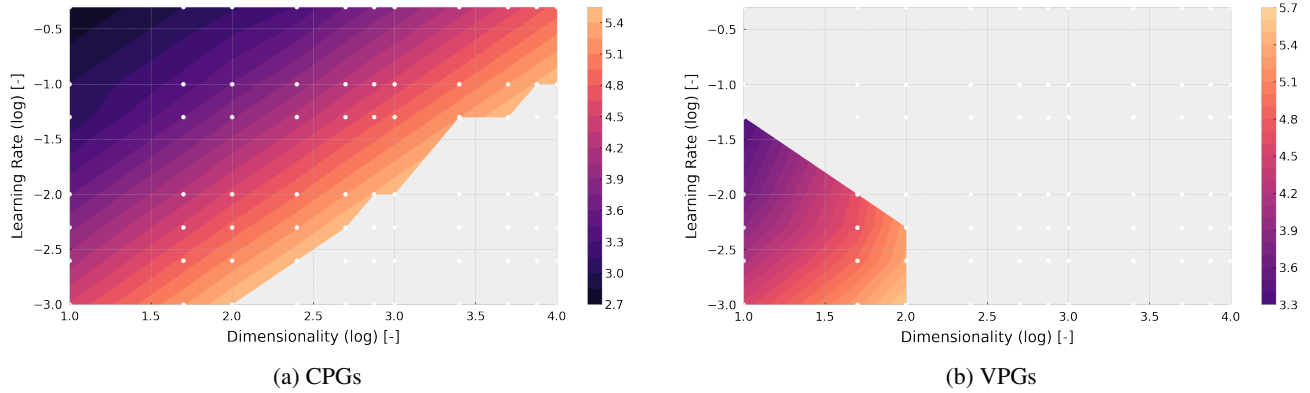


Figure 9. Mean number of time steps required to reach an optimality gap of 0.1, up to a limit of 5×10^5 training iterations; see [Figure 4](#). The z -axis is given in a log scale, and unfilled (grey) regions depict either divergence or a failure to terminate in the allotted time. Each point was computed from 16 random samples under the assumption of a Gamma distribution (time is lower bounded at zero).

B. Apples and Oranges

The apples and oranges domain is practically-motivated problem environment in which CPGs has a very natural application. Indeed, many important classes of problems in finance, retail, advertising, and customer interaction (i.e. settings which are highly concurrent) exhibit this very structure. As shown in [Figure 11](#), the influence diagram has a clear delineation between apples and oranges — unsurprisingly — and justifies the use of two policies under minimum factorisation; as discussion in [Section 5.1](#). In industry, problems of this form grow very large, very quickly, and the need for scalable RL techniques cannot be understated.

In our experiments we used the following configuration of hyperparameters based on `rllib`’s implementation of PPO using GAE and state-dependent baselines:

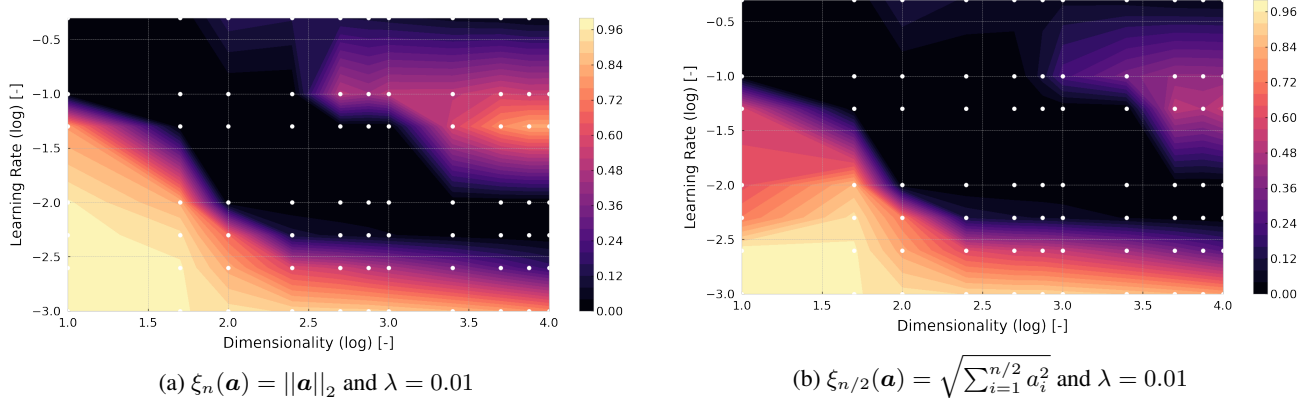


Figure 10. Ratio between the mean optimality gaps for CPGs over VPGs after 2×10^5 training iterations. Smaller values indicate that CPGs achieved a lower error relative to VPGs. Each point is the ratio of the two means, each computed using 16 random samples under the assumption of a Gamma distribution (optimality gaps are lower bounded at zero).

Time horizon The problem is infinite-horizon, therefore we set `no_done_at_end` to be `True`, and the discount factor was set as $\gamma \doteq 0.99$.

Learning rate The step-size used during the SGD updates was set at $\alpha \doteq 5 \times 10^{-5}$ with minibatch-size of 128 for each of 30 iterations.

Policy network Each policy factor (regardless of output/input size) was modelled as a two-layer, fully-connected neural network with tanh activation functions. Each hidden layer was initialised with 256 nodes using `tensorflow` as the underlying implementation.

Advantage estimation As mentioned, GAE was used to estimate the advantage used in updating the policy. We used a value $\lambda \doteq 1$ such that the target corresponded to the full Monte-Carlo returns.

PPO PPO itself has a number of parameters for which we used the following configuration: value function loss coefficient $c_1 \doteq 10$; an entropy bonus coefficient of $c_2 \doteq 0$; reward clipping at $\epsilon_r \doteq 0.3$ and value clipping at $\epsilon_v \doteq 10$; a KL divergence target of $d_{\text{targ}} \doteq 0.01$.

For more details, see the documentation for PPO that is available on the website hosted by `rllib`. The version used in our experiments was `1.1.0`. The environmental parameters were also set as follows:

Demand processes The demand for each fruit was modelled as a zero-inflated Poisson distribution. The null-probability is given in the text, but the rates were set at $\lambda_A \doteq 15$ and $\lambda_O \doteq 20$ for apples and oranges respectively.

Market prices At market, apples and oranges were assigned the retail values of $u_A \doteq 5$ and $u_O \doteq 4$, respectively.

Wholesalers The wholesalers were initialised such that

$$\begin{aligned} \mathbf{c}_A &= (3.75, 3.82, 4.85, 4.67, 4.76), \\ \mathbf{c}_O &= (3.73, 3.40, 4.44, 3.32, 3.26), \end{aligned}$$

with maximum order sizes of $\bar{a}_A \doteq 8$ and $\bar{a}_O \doteq 10$.

C. Supplementary Lemmas

Lemma C.1 (Control Variate). *Let X , Y and Z be random variables where the law of X conditional on Z is denoted $\mathbb{P}_\theta(X|Z)$, and Y is independent of X conditioned on Z ; i.e. $X \perp\!\!\!\perp Y \mid Z$. Then, we have that $\mathbb{E}[Y \nabla_\theta \ln \mathbb{P}_\theta(X)] = 0$.*

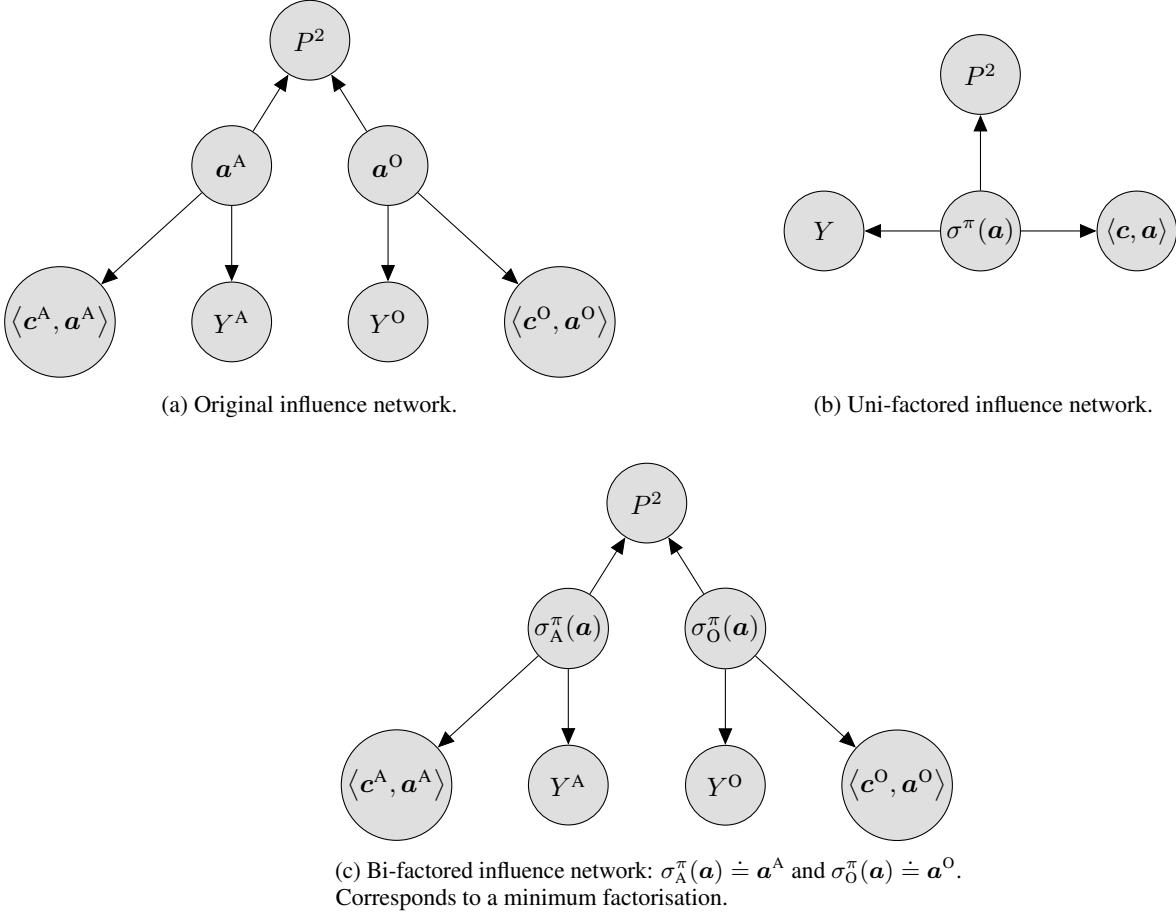


Figure 11. Influence networks for the apples and oranges problem in terms of the rewards components, including the income, cost and (coupled) spoilage penalty. Note that the actual algorithm uses targets that are defined as the expected discounted sum of future values for each of these terms.

Proof. The proof follows from the law of iterated expectations:

$$\mathbb{E}[Y \nabla_{\theta} \ln \mathbb{P}_{\theta}(X)] = \mathbb{E}[\mathbb{E}[Y \nabla_{\theta} \ln \mathbb{P}_{\theta}(X) | Z]] = \mathbb{E}[\mathbb{E}[Y | Z] \mathbb{E}[\nabla_{\theta} \ln \mathbb{P}_{\theta}(X) | Z]] = 0,$$

since $\mathbb{E}[\nabla_{\theta} \ln \mathbb{P}_{\theta}(X) | Z] = 0$. ■

D. Details of Lemma 4.1

D.1. Proof

Consider an objective $J(\theta)$ of the form defined in Equation 4, a factored influence network \mathcal{G}_{Σ} and a Σ -factored policy $\pi_{\theta}(a | s) \doteq \prod_{i=1}^n \pi_{i,\theta}(\sigma_i^\pi(a) | s)$. Now, let us define a stochastic policy gradient estimator

$$\nabla_{\theta} J(\theta) = \mathbb{E}_{\pi_{\theta}, \rho_{\pi_{\theta}}} \left[g(s, a) \doteq \sum_{i=1}^n [\psi(s, a) + b_i^C(s, \bar{\sigma}_i^\pi(a))] z_i \right],$$

where $z_i \doteq \nabla_{\theta} \ln \pi_{i,\theta}(\sigma_i^\pi(a) | s)$ and $b_i^C(s, \bar{\sigma}_i^\pi(a))$ is the i^{th} causal baseline (see Definition 4.1). Now, since $b_i^C(s, \bar{\sigma}_i^\pi(a))$ depends only on s and $\bar{\sigma}_i^\pi(a)$ — i.e. the action elements that are not in the support of $\pi_{i,\theta}$ — we can readily apply Lemma C.1, concluding the proof. ■

D.2. Optimal Baseline Discussion

Solving for the optimal baseline is a non-trivial challenge in full generality. Indeed, the results presented by Wu et al. (2018) rely on a key assumption that the policy factors do not share parameters in order to simplify the analysis; i.e. that $\langle \mathbf{z}_i, \mathbf{z}_j \rangle \approx 0$ for any $i, j \in [|\Sigma|]$. Below we explain why this is a difficult problem, and leave it to future work to find the solution.

For notational convenience, let $\mathbf{g}(s, \mathbf{a}) \doteq \sum_{i=1}^n \mathbf{g}_i(s, \mathbf{a})$ such that the total variance on the gradient is given by

$$\mathbb{V}[\mathbf{g}(s, \mathbf{a})] = \sum_{i=1}^n \sum_{j=1}^n \text{Cov}[\mathbf{g}_i(s, \mathbf{a}), \mathbf{g}_j(s, \mathbf{a})]. \quad (11)$$

The n optimal baselines are given by the values that minimise Equation 11; i.e. $b_i^*(s, \bar{\sigma}_i^\pi(\mathbf{a})) \doteq \arg \min_{b_i} \mathbb{V}[\mathbf{g}(s, \mathbf{a})]$ for all $i \in [n]$. To solve this problem, we first apply the causal baseline decomposition such that $b_i^*(s, \bar{\sigma}_i^\pi(\mathbf{a})) = b_i^V(s, \bar{\sigma}_i^\pi(\mathbf{a})) + b_i^C(s, \bar{\sigma}_i^\pi(\mathbf{a}))$. This implies that the optimisation problem can be reduced to finding $\arg \min_{b_i^V} \mathbb{V}[\mathbf{g}(s, \mathbf{a})]$ when b_i is replaced with b_i^* for all $i \in [n]$. Now, let $\mathbf{x}_i \doteq [\mathbf{K}_\Sigma \boldsymbol{\psi}(s, \mathbf{a})]_i \mathbf{z}_i$ and $\mathbf{y}_i \doteq b_i^V(s, \bar{\sigma}_i^\pi(\mathbf{a})) \mathbf{z}_i$ such that $\mathbf{g}_i(s, \mathbf{a}) = \mathbf{x}_i + \mathbf{y}_i$. Note that while \mathbf{y}_i depends on the full action, \mathbf{x}_i depends only on the actions influencing the targets in $[\mathbf{K}_\Sigma \boldsymbol{\psi}(s, \mathbf{a})]_i$. Removing terms that are independent of b_i^V thus yields the following:

$$\begin{aligned} \arg \min_{b_i^V} \mathbb{V}[\mathbf{g}] &= \arg \min_{b_i^V} \left\{ \mathbb{V}[\mathbf{g}_i] + \sum_{j \neq i}^n \text{Cov}[\mathbf{g}_i, \mathbf{g}_j] \right\}, \\ &= \arg \min_{b_i^V} \left\{ \mathbb{V}[\mathbf{x}_i] + \mathbb{V}[\mathbf{y}_i] + 2 \text{Cov}[\mathbf{x}_i, \mathbf{y}_i] + \sum_{j \neq i}^n \text{Cov}[\mathbf{x}_i, \mathbf{x}_j] + \text{Cov}[\mathbf{x}_i, \mathbf{y}_j] + \text{Cov}[\mathbf{y}_i, \mathbf{x}_j] + \text{Cov}[\mathbf{y}_i, \mathbf{y}_j] \right\}, \\ &= \arg \min_{b_i^V} \left\{ \mathbb{V}[\mathbf{y}_i] + 2 \text{Cov}[\mathbf{x}_i, \mathbf{y}_i] + \sum_{j \neq i}^n \text{Cov}[\mathbf{x}_i, \mathbf{y}_j] + \text{Cov}[\mathbf{y}_i, \mathbf{x}_j] + \text{Cov}[\mathbf{y}_i, \mathbf{y}_j] \right\}. \end{aligned}$$

To solve the equation above, we first expand each component and remove any redundant terms. For the variance on \mathbf{y}_i , we have that

$$\begin{aligned} \mathbb{V}[\mathbf{y}_i] &= \mathbb{E}_{\mathbf{a}} \left[(b_i^V)^2 \langle \mathbf{z}_i, \mathbf{z}_i \rangle \right] + \langle \mathbb{E}_{\mathbf{a}} [b_i^V \mathbf{z}_i], \mathbb{E}_{\mathbf{a}} [b_i^V \mathbf{z}_i] \rangle, \\ &= \mathbb{E}_{\mathbf{a}} \left[(b_i^V)^2 \langle \mathbf{z}_i, \mathbf{z}_i \rangle \right] + \langle \mathbb{E}_{\bar{\sigma}_i^\pi(\mathbf{a})} [b_i^V] \mathbb{E}_{\sigma_i^\pi(\mathbf{a})} [\mathbf{z}_i], \mathbb{E}_{\bar{\sigma}_i^\pi(\mathbf{a})} [b_i^V] \mathbb{E}_{\sigma_i^\pi(\mathbf{a})} [\mathbf{z}_i] \rangle, \\ &= \mathbb{E}_{\mathbf{a}} \left[(b_i^V)^2 \langle \mathbf{z}_i, \mathbf{z}_i \rangle \right], \\ &= \mathbb{E}_{\sigma_i^\pi(\mathbf{a})} [\langle \mathbf{z}_i, \mathbf{z}_i \rangle] \mathbb{E}_{\bar{\sigma}_i^\pi(\mathbf{a})} [(b_i^V)^2]. \end{aligned} \quad (12)$$

It follows from this analysis that the covariance between \mathbf{y}_i and \mathbf{y}_j for any $i, j \in [|\Sigma|]$, with $i \neq j$, is given by

$$\text{Cov}[\mathbf{y}_i, \mathbf{y}_j] = \mathbb{E}_{\mathbf{a}} [b_i^V b_j^V \langle \mathbf{z}_i, \mathbf{z}_j \rangle]. \quad (13)$$

Finally, we can expand the covariance between \mathbf{x}_i and \mathbf{y}_i ,

$$\begin{aligned} \text{Cov}[\mathbf{x}_i, \mathbf{y}_i] &= \mathbb{E}_{\mathbf{a}} [\mathbf{K}_\Sigma \boldsymbol{\psi}]_i b_i^V \langle \mathbf{z}_i, \mathbf{z}_i \rangle + \langle \mathbb{E}_{\mathbf{a}} [\mathbf{K}_\Sigma \boldsymbol{\psi}]_i \mathbf{z}_i, \mathbb{E}_{\mathbf{a}} [b_i^V \mathbf{z}_i] \rangle, \\ &= \mathbb{E}_{\mathbf{a}} [\mathbf{K}_\Sigma \boldsymbol{\psi}]_i b_i^V \langle \mathbf{z}_i, \mathbf{z}_i \rangle + \langle \mathbb{E}_{\mathbf{a}} [\mathbf{K}_\Sigma \boldsymbol{\psi}]_i \mathbf{z}_i, \mathbb{E}_{\bar{\sigma}_i^\pi(\mathbf{a})} [b_i^V] \mathbb{E}_{\sigma_i^\pi(\mathbf{a})} [\mathbf{z}_i] \rangle, \\ &= \mathbb{E}_{\mathbf{a}} [\mathbf{K}_\Sigma \boldsymbol{\psi}]_i b_i^V \langle \mathbf{z}_i, \mathbf{z}_i \rangle, \\ &= \mathbb{E}_{\bar{\sigma}_i^\pi(\mathbf{a})} [b_i^V] \mathbb{E}_{\sigma_i^\pi(\mathbf{a})} [\mathbf{K}_\Sigma \boldsymbol{\psi}]_i \langle \mathbf{z}_i, \mathbf{z}_i \rangle, \end{aligned} \quad (14)$$

and similarly resolve the cross-covariance terms:

$$\text{Cov}[\mathbf{x}_i, \mathbf{y}_j] = \langle \mathbb{E}_{\bar{\sigma}_i^\pi(\mathbf{a})} [b_i^V \mathbf{z}_i], \mathbb{E}_{\sigma_j^\pi(\mathbf{a})} [\mathbf{K}_\Sigma \boldsymbol{\psi}]_j \mathbf{z}_j \rangle. \quad (15)$$

The quantities above provide us with a platform to find solutions. For example, the optimal baseline approximation proposed by Wu et al. (2018) can be found if we assume that $\langle z_i, z_j \rangle \approx 0$ since Equation 13 and Equation 14 go to zero. However, in the general case the problem is not quite so simple. The reason for this is that the baselines interact via the cross-covariance term in Equation 13. As a result, we cannot solve for each b_i^V independently of the others. Instead, we have a system of polynomial equations which may not have a unique solution. In fact, since each equation has degree $d = 2$, it follows the number of solutions can be as large $d^{|\Sigma|}$. In general, there are very few methods that can solve these type of systems, and those that can are limited to bounds of approximately $d^{|\Sigma|} \approx 20$. It seems reasonable to assume that any solution, while viable, would be computationally impractical, but we leave it to future work to establish this result formally.

E. Proof of Proposition 1

Let \mathcal{G}_Σ denote an Σ -factored influence network with policy $\pi_\theta(\mathbf{a} | s) \doteq \prod_{i=1}^n \pi_{i,\theta}(\sigma_i^\pi(\mathbf{a}) | s)$, and global target function $\psi(s, \mathbf{a}) = \sum_{j=1}^m \lambda_j \psi_j(s, \sigma_j(\mathbf{a})) = \langle \boldsymbol{\lambda}, \boldsymbol{\psi}(s, \mathbf{a}) \rangle$. The score matrix, $\mathbf{S}(s, \mathbf{a}) \doteq [\mathbf{z}_1^\top, \dots, \mathbf{z}_n^\top]^\top$, then has size $|\theta| \times n$, where $\mathbf{z}_i \doteq \nabla_\theta \ln \pi_{i,\theta}(\sigma_i^\pi(\mathbf{a}) | s)$. From this we can express the conventional policy gradient with no baseline as the linear product $\mathbf{g}(s, \mathbf{a}) = \mathbf{S}(s, \mathbf{a}) \mathbf{J}_{n,m} \boldsymbol{\psi}(s, \mathbf{a})$, where $\mathbf{J}_{n,m}$ is the $n \times m$ all-ones matrix. By Lemma 4.1 the causal baselines, $[(1 - \mathbf{K}_\Sigma) \boldsymbol{\psi}(s, \mathbf{a})]_i$, are valid control variates and thus have expected value of zero under π . This means that they can be subtracted without introducing bias in the policy gradient, yielding

$$\mathbf{g}(s, \mathbf{a}) = \underbrace{\mathbf{S}(s, \mathbf{a}) \mathbf{J}_{n,m} \boldsymbol{\psi}(s, \mathbf{a})}_{\text{Vanilla PG}} - \underbrace{\mathbf{S}(s, \mathbf{a}) (1 - \mathbf{K}_\Sigma) \boldsymbol{\psi}(s, \mathbf{a})}_{\text{Causal Correction}} = \mathbf{S}(s, \mathbf{a}) \mathbf{K}_\Sigma \boldsymbol{\psi}(s, \mathbf{a}).$$

It follows that $\nabla_\theta J(\theta) = \mathbb{E}_{\pi_\theta, \rho_{\pi_\theta}} [\mathbf{g}^C(s, \mathbf{a})]$ since $\mathbb{E}_{\pi_\theta, \rho_{\pi_\theta}} [\mathbf{g}^V(s, \mathbf{a})] = \mathbb{E}_{\pi_\theta, \rho_{\pi_\theta}} [\mathbf{g}^C(s, \mathbf{a})]$ which concludes the proof. ■

F. Proof of Proposition 2

First, let us denote by \mathbf{X} and \mathbf{Y} two (possibly dependent) random variables, with $\mathbf{Z} \doteq \mathbf{X} - \mathbf{Y}$ such that

$$\begin{aligned} \Delta \mathbb{V} &\doteq \mathbb{V}[\mathbf{X}] - \mathbb{V}[\mathbf{Y}] = \mathbb{V}[\mathbf{Z} + \mathbf{Y}] - \mathbb{V}[\mathbf{Y}], \\ &= \mathbb{V}[\mathbf{Z}] + \mathbb{V}[\mathbf{Y}] + 2\text{Cov}[\mathbf{Y}, \mathbf{Z}] - \mathbb{V}[\mathbf{Y}], \\ &= \mathbb{V}[\mathbf{Z}] + 2\text{Cov}[\mathbf{Y}, \mathbf{Z}]. \end{aligned}$$

From Proposition 1, we can express the vanilla and causal policy gradient estimators for the i^{th} factor as $\psi \mathbf{S}_{\cdot,i}$ and $(\psi - b_i^C) \mathbf{S}_{\cdot,i}$, respectively, where the function arguments have been omitted for clarity. Assigning these values to \mathbf{X} and \mathbf{Y} we arrive at the equality relations

$$\begin{aligned} \mathbb{V}[\mathbf{Z}] &= \mathbb{V}[b_i^C \mathbf{z}_i] = \mathbb{E}_\pi [\langle \mathbf{z}_i, \mathbf{z}_i \rangle (b_i^C)^2] \\ \text{Cov}[\mathbf{Y}, \mathbf{Z}] &= \text{Cov}[(\psi - b_i^C) \mathbf{z}_i, b_i^C \mathbf{z}_i] = \mathbb{E}_\pi [\langle \mathbf{z}_i, \mathbf{z}_i \rangle (\psi - b_i^C) b_i^C]. \end{aligned}$$

The former follows from the fact that $\mathbb{E}_\pi[\mathbf{S}_{\cdot,i}] = 0$ for all i , and latter by noting that $\mathbb{E}[\mathbf{Z}] = 0$ due to Lemma 4.1. We can now exploit the independencies implied by the influence network, \mathcal{G}_Σ , to give

$$\Delta \mathbb{V}_i = \mathbb{E}_{\sigma_i^\pi(\mathbf{a})} [\langle \mathbf{z}_i, \mathbf{z}_i \rangle] \mathbb{E}_{\bar{\sigma}_i^\pi(\mathbf{a})} [(b_i^C)^2] + 2\mathbb{E}_{\sigma_i^\pi(\mathbf{a})} [\langle \mathbf{z}_i, \mathbf{z}_i \rangle (\psi - b_i^C)] \mathbb{E}_{\bar{\sigma}_i^\pi(\mathbf{a})} [b_i^C],$$

This is the desired result and thus concludes the proof. ■

G. Proof of Corollary 4.1

Take a target set Ψ and let $\psi_j \doteq \inf_{S, \mathcal{A}} \psi_j$ for each $\psi \in \Psi$. The unbiasedness claim follows from the fact that these terms go to zero in expectation when weighted by the score functions; they are constants. The variance claim is also trivial, since $\psi_j + \sum_{k=1}^m \lambda_k \inf_{S, \mathcal{A}} \psi_k$ are non-negative and, due to the summation over all $k \in [m]$, no CB can yield a negative value. Each term in Equation 9 (Proposition 2) must also be non-negative, which concludes the proof. ■

H. Proof of Theorem 5.1

First, note that bipartite graphs always have at least one valid biclique and thus MF. Now, for uniqueness, let \mathcal{G} denote an influence network. If \mathcal{G} is complete, then we automatically satisfy the uniqueness property since the MF will contain a single biclique that covers all vertices in I_A . If \mathcal{G} is incomplete, then the proof can be shown through contradiction. Suppose that A and B are both MFs and therefore correspond to minimum biclique vertex covers, disjoint amongst I_A . We know then that A and B must have the same dimensionality since they are optimal — i.e. contain the same number of bicliques — but, if they are distinct, then there must also exist at least one biclique $a \in A$ that is not in B . Since both MFs are defined over the same graph \mathcal{G} , the elements of a must be distributed between at least 2 distinct bicliques in B . However, if this is the case, the union of these subgraphs would also form a valid biclique. The new cover, B' , containing the merged bicliques is valid and has dimensionality $|B'| < |B| = |A|$. This implies that neither A nor B can be MFs. Since the same must be true for any A and B , it follows that there can be only one MF, thus concluding the proof. ■